Supporting Information

Fujimura et al. 10.1073/pnas.1310750111

SI Materials and Methods

House Dust Collection. Dust from homes with or without dogs was collected using a sterile fabric filter sock inserted into a sterile vacuum nozzle immediately before vacuuming a 3′ × 3′ area for 3 min. The sock was removed from the vacuum, the collected dust weighed and sieved through a 300-μm sieve to remove large debris from the sample. Comparable sieved samples have previously been used successfully to profile microbial communities present in house dust (1, 2). Dust samples were subsequently divided into 25- or 6.25-mg fractions for dog (D)- or no-pet (NP)-associated houses, respectively, each stored in a sterile 5-mL tube at −20 °C until used for murine supplementation.

Murine Models. ***Cockroach allergen model.*** BALB/c were purchased from The Jackson Laboratory. On the day of use, a single tube of dust was resuspended in sterile saline (1 mL) and immediately administered by oral gavage to animals (100-μL supplementation per mouse); one group of control animals received sterile saline, the other, no supplement. This procedure ensured that animals received standardized (by weight) quantities of dust throughout the duration of the study and that dust samples were not impacted by recurrent freeze–thaw cycles. Supplementation was performed daily for 7 d before initial cockroach allergen extract (CRA) sensitization, and twice per week for the following 2 wk. CRA (Hollister-Stier) sensitization was performed as previously described (3). Briefly, 6- to 8-wk-old female mice were sensitized to CRA by three consecutive intratracheal instillations (5 μg in 50 μL) on days 0, 1, and 2. On days 14, 20, and 22, mice were locally challenged with CRA by intratracheal route, and mice were euthanized at day 23 (Fig. S1*A*).

For experiments examining whether inoculum level impacted airway immune responses, animals were supplemented with either 25 mg of D or NP dust [high dust exposure (HD)] or to 6.25 mg of D or NP dust [low dust exposure (LD)] daily as described above.

OVA allergen model. In this model, we again exposed BALB/c mice to dust from D- or NP-containing homes (or *Lactobacillus johnsonii*, see below) by oral gavage as described above. CD4 splenic T cells from DO.11 ovalbumin TCR-specific mice were purified by negative selection using CD4 T-Cell Isolation Kit (Miltenyi Biotec) according to the manufacturer's instructions. On day 14, naïve carboxyfluorescein succinimidyl ester (CFSE)-labeled splenic $CD4^+$ T cells isolated from DO.11 OVA peptide-specific T-cell receptor transgenic mice (1×10^6 cells·mouse^{-1}; obtained from The Jackson Laboratory) were transferred via tail vein injection. One day after T-cell transfer, animals were challenged with whole ovalbumin protein (350 μg) into the airway. Three days later, mice were killed, and lungs and lymph nodes were harvested (Fig. S1*B*).

Respiratory syncytial virus infection. Our laboratory uses antigenic subgroup A, line 19 respiratory syncytial virus (RSV), originally obtained from a sick infant at the University of Michigan. Infection with this RSV isolate for 8 d recapitulates several aspects of human infection including inflammatory responses, T-cell–mediated pathology, and airway mucus production upon intratracheal infection with 1×10^5 pfu/mouse (4).

Lung Histology. The left lung was perfused with 4% (vol/vol) formaldehyde for fixation and embedded in paraffin. Five-micrometer lung sections were stained with periodic acid-Schiff and H&E to detect mucus production and inflammatory infiltrates, respectively. Photomicrographs were captured using a Zeiss Axio Imager Z1 and AxioVision 4.8 software (Zeiss).

mRNA Extraction, Reverse Transcription, and RT-PCR. mRNA was isolated from ground lung tissue using TRIzol reagent (Invitrogen) or the RNeasy Mini kit (Qiagen) according to manufacturer's instructions. A total of 5 μg of RNA per sample was reverse transcribed using murine leukemia virus RTase (Applied Biosystems). Expression of relevant genes was analyzed with TaqMan gene expression assays (Applied Biosystems) using an ABI Prism 7500 Sequence Detection System (Applied Biosystems). Gene expression was normalized to GAPDH and expressed as fold change over expression in control mice.

Culture and Stimulation of Lymph Node Cells. Mediastinal lymph nodes were digested mechanically, using 18-gauge needles, and enzymatically, via incubation with 1 mg/mL Collagenase A (Roche) and DNase I (Sigma-Aldrich) in RPMI 1640 with 10% FCS. Following red blood cell lysis, cells were passed through a 40-μm strainer and counted with a Z2 Beckman Coulter particle counter. Suspensions of total lymph node cells were cultured in complete medium and restimulated with CRA for 48 h or with OVA (100 μg·ml^{-1}) for 96 h. Levels of T-helper cytokines, IL-4, IL-5, IL-13, IFNγ, and IL-17 were determined in culture supernatants using a Bio-Plex assay (Bio-Rad). The remainder of the lymph node cells was analyzed using flow cytometry.

Flow Cytometry. Following FcR blocking, single-cell suspensions of BAL, lung, and lymph node cells were stained with anti-CD11c (N418), anti-Ly6C (HK1.4), anti-Ly6G (1A8; Biolegend), anti-CD11b (M1/70), anti-CD103 (2E7) (eBioscience), and anti-MHC-II/IAb (AF6-120.1; BD Biosciences). Inflammatory neutrophils were gated as low autofluorescent, $CD11c^{lo}CD11b^{hi}Ly6C^+Ly6G^+$ with low forward scatter. Inflammatory monocytes were analyzed as low autofluorescent, $CD11c^{lo}CD11b^{hi}Ly6C^+Ly6G^-$ cells with low forward scatter. $CD11b^+$ dendritic cells were defined as low autofluorescent, $CD11c^{hi}MHCII^+CD11b^{hi}CD103^-$ cells; within this population, $Ly6C^+$ cells were considered to be inflammatory $CD11b^+$ DCs. $CD103^+$ dendritic cells were defined as low autofluorescent, $CD11c^{hi}MHCII^+CD11b^{lo}CD103^+$ cells. Upon staining for surface markers with anti-CD3 (17A2), anti-CD4 (RM4-5), anti-CD8 Abs (16-10A1; Biolegend), and anti-CD69 Ab (H1.2F3; eBioscience), T cells were defined as CD3-positive cells with low forward and side scatter, and subdivided into CD4 or CD8 single-positive subpopulations, using CD69 expression as a marker of early activation.

Cecal Microbiome Profiling. Dust samples were extracted using a cetyltrimethylammonium bromide (CTAB)–polyethylene glycol (PEG) protocol as previously described (5). Briefly, 0.5 mL of modified CTAB extraction buffer [1:1 10% CTAB in 1 M NaCl to 0.5 M phosphate buffer (pH 7.5–8) in 1 M NaCl] were added to 0.2 g of dust (when available) in Lysing Matrix E tubes (MP Biomedicals), followed by 500 μL of phenol:cholorform:isoamyl alcohol (25:24:1). Samples were bead-beaten using MPBio FastPrep-24 at 5.5 m/s for 30 s before centrifugation for 5 min at 16,000 × *g* at 4 °C. The supernatant was then transferred to heavy phase-lock gel 1.5-mL tubes (5Prime). One volume of chloroform was added to each sample and centrifuged for 5 min at 12,000 × *g* at 4 °C. An additional 0.5 mL of CTAB-modified extraction buffer was added to each lysing matrix tube to increase recovery of nucleic acid from each sample. One microliter of linear acrylamide was added to the extracted supernatant

followed by 2 vol of PEG. Following a 2-h incubation at room temperature, samples were washed with ice-cold 70% ethanol and resuspended in 30 μL of molecular-grade H_2O. Extracted material was pooled for each sample before application to the DNA column of the Qiagen AllPrep DNA/RNA extraction kit, and DNA was extracted according to the manufacturer's instructions.

Cecal samples were harvested immediately after the animals were sacked, placed in RNAlater (Life Technologies), and stored for 24 h at 4 °C, before storage at −80 °C until processed for microbiome profiling. Frozen cecal samples were thawed on ice and transferred into individual Lysing Matrix E tubes (MP Biomedicals) containing 600 μL of RLT^+ buffer (Qiagen). Samples were bead-beaten for 30 s at 5.5 m/s using MPBio FastPrep-24 (MP Biomedicals), centrifuged for 1 min at 2,000 rpm (Eppendorf 5424R microcentrifuge), and transferred to the AllPrep Kit (Qiagen) for DNA extraction following the manufacturer's protocol.

PCR reactions for PhyloChip analysis were performed in 25-μL reactions using 0.02 U of Takara ExTaq (Takara Mirus Bio), 1× Takara buffer with $MgCl_2$, 0.3 pmol·μL^{-1} of 27F and 1492R primer (Lane 1991), 0.8 mM dNTPs, 0.8 mg·mL^{-1} BSA (Roche Applied Science), and 30 ng of DNA template. A total of 12 reactions per sample were performed in an Eppendorf Mastercycler gradient thermocycler across a gradient (48–58.4 °C) of annealing temperatures to maximize diversity recovered. Reaction conditions were as follows: initial denaturation (95 °C for 3 min) followed by 25 cycles of 95 °C (30 s), annealing (30 s), and extension at 72 °C (2 min), and a final extension of 72 °C (10 min). PCR amplification was verified using a 1% TBE agarose gel.

PhyloChip Profiling. Amplified 16S rRNA product was purified using the QIAquick Gel Extraction Kit (Qiagen) before being pooled, fragmented, and biotinylated. A total of 250 ng of labeled amplicon per sample containing quantitative standards (consisting of 14 non-16S rRNA genes that permit data normalization) was applied to each G2 PhyloChip (Affymetrix). Arrays were processed as previously described (2).

***L. johnsonii* Isolation and Identification.** Ceca from four mice gavaged with D-associated house dust were extracted aseptically from animals. Cecal contents were removed under aseptic conditions, transferred into 500 μL of sterile PBS, and vortexed vigorously for 1 min to resuspend. Suspensions were serially diluted 10-fold in sterile PBS, and 10^{-2} to 10^{-5} dilutions were plated on *Lactobacillus* selective de Man, Rogosa and Sharpe (MRS) agar (BD Biosciences). For each of the four cecal samples, six colonies were selected for further analysis from the lowest serial dilution that yielded individual colonies. Identity was determined by full-length bidirectional Sanger sequencing (University of California, San Francisco, Genomics Core Facility) of the 16S rRNA gene. Overlapping contigs for each clone were assembled in Codon Code Aligner (CodonCode Corporation), and the resulting 21 high-quality consensus sequences were interrogated using both BLAST (National Center for Biotechnology Information; http://blast.ncbi.nlm.nih.gov/Blast.cgi) and the 16S rRNA Greengenes database (6).

Generation of *L. johnsonii* Supplements for Murine Studies. To generate supplements with 5×10^7 CFU per 100 μL, 100 mL of MRS broth was inoculated with *L. johnsonii* from a glycerol stock before static overnight culture at 37 °C. Stationary-phase cells (OD_{600} = 0.89) were centrifuged at 4,000 rpm (Eppendorf 5424R microcentrifuge) for 15 min at 4 °C and resuspended in 60 mL of a 50:50 (vol/vol) solution of MRS broth/50% glycerol. Cells were aliquoted into batches of 500 μL, snap frozen in liquid nitrogen, and stored at −80 °C until they were used in murine studies. Viable cell count of the glycerol stock was determined to be 2.7×10^8 CFU per vial. For murine supplementation studies, tubes were defrosted on ice, centrifuged at 14,000 rpm (Eppendorf 5424R microcentrifuge) for 30 s at 4 °C, and washed twice in sterile saline to remove excess glycerol. The cells were then resuspended in 700 μL of sterile saline. Each mouse received 100 μL (equivalent to 3.9×10^7 CFU) of resuspended *L. johnsonii*. The remaining suspension was plated on MRS media to confirm that viable *L. johnsonii* cell counts remained high and stable throughout the duration of the study.

Validation of *L. johnsonii* Presence by Q-PCR. Quantitative PCR (Q-PCR) was used to validate *L. johnsonii* relative abundance reported by the by the array using the QuantiTect SYBR Green PCR kit per the manufacturer's instructions (Qiagen) and the *L. johnsonii*-specific primer pair Lj1 and La2 (7). A total of 10 ng of DNA extracted from cecal samples per reaction was used in triplicate, 25-μL Q-PCR reactions at an annealing temperature of 60 °C. Inverse cycle threshold values were plotted against array fluorescence intensity. Correlation using cor.test in R (www.R-project.org) was calculated to assess concordance between the two independent molecular methods.

Statistical Analyses. As an exploratory tool to examine community composition dissimilarity, nonmetric multidimensional scaling (NMDS) or principal coordinate analysis (PCoA) was performed, based on Canberra (8) or UniFrac (9) distance matrices, respectively. PhyloChip fluorescence intensities, normalized to quantitative standards were $\log_2 \times 1{,}000$ transformed before analyses. Canberra distance matrix was generated in R (www.R-project.org). The stepacross dissimilarity between shared species (noshare) was set at 0.1, and the maximum number of random starts was set at 30 in the *vegan* package. NMDS was conducted using the default settings for metaMDS. PCoA was performed using a UniFrac distance matrix and cmdscale in *stats* and constructed using the *ade4* package (10). The percentage of variability explained by the two axes was calculated by dividing the eigenvalue for each axis by the sum of all positive eigenvalues.

Community richness was determined in a two-stage process where probe sets were scored (r) by the potential of the probe pair to respond to the target and not to the background; for each r score, a minimum of 18 probe pairs were considered (11). For an operational taxonomic unit (OTU) to be considered present, the r score was required to pass the following three thresholds: $rQ_1 \geq 0.379$, $rQ_2 \geq 0.565$, and $rQ_3 \geq 0.82$. OTUs that passed this first stage of data filtration were then considered for stage 2, where $r_{subx} \geq 0.5$ (11). Pielou's evenness was calculated using the *vegan* package, and Faith's phylogenetic diversity was determined using the *picante* package. Kruskal–Wallis, nonparametric ANOVA, in *stats* was used to test whether significant differences existed between treatment groups. Student's, Wilcoxon, or Welch's *t* test was used to determine significant differences between pairs of treatment groups as appropriate. *Q*-value false-discovery rates were calculated as previously described (12) when multiple comparisons were made. Values of P and $q > 0.05$ and 0.15, respectively, were considered significant. Phylogenetic trees were constructed in iTOL (13, 14).

In Silico Metagenome Prediction. PICRUSt (Phylogenetics Investigation of Communities by Reconstruction of Unobserved States), a bioinformatics software used to predict functional metagenomes from a marker gene survey (such as 16S rRNA gene) (http://picrust.github.com/picrust/), was used to generate in silico metagenomes for data generated in this study. First, 16S rRNA sequences were obtained for OTUs significantly enriched in the cecal microbiota of D-associated house dust- and *L. johnsonii*-supplemented animals (compared with respective control animals) by PhyloChip from the GreenGenes database (http://greengenes.secondgenome.com/downloads/database/13_5) using a custom script written in Python. Retrieved 16S rRNA sequences were

imported into QIIME to generate an OTU table, through a closed-referenced OTU-picking protocol. This OTU table was then subjected to PICRUSt analysis and grouped into corresponding KEGG pathways using the KEGG database (www.genome.jp/kegg/pathway.html). Comparisons between D dust- or *L. johnsonii*-supplemented animals and their relative controls were visualized using a heat map constructed using a custom script written in R, to indicate, based on presence–absence data, the KEGG pathways enriched in each respective group. The custom pipeline developed to analyze and visualize this data are open source and available at GitHub (https://github.com/alifar76/PHoP).

1. Fujimura KE, et al. (2012) Development of a standardized approach for environmental microbiota investigations related to asthma development in children. *J Microbiol Methods* 91(2):231–239.
2. Fujimura KE, et al. (2010) Man's best friend? The effect of pet ownership on house dust microbial communities. *J Allergy Clin Immunol* 126(2), 410–412, 412.e1–3.
3. Berlin AA, Hogaboam CM, Lukacs NW (2006) Inhibition of SCF attenuates peribronchial remodeling in chronic cockroach allergen-induced asthma. *Lab Invest* 86(6):557–565.
4. Demoor T, et al. (2012) IPS-1 signaling has a nonredundant role in mediating antiviral responses and the clearance of respiratory syncytial virus. *J Immunol* 189(12):5942–5953.
5. DeAngelis KM, et al. (2009) Selective progressive response of soil microbial community to wild oat roots. *ISME J* 3(2):168–178.
6. DeSantis TZ, et al. (2006) Greengenes, a chimera-checked 16S rRNA gene database and workbench compatible with ARB. *Appl Environ Microbiol* 72(7):5069–5072.
7. Furet JP, Quénée P, Tailliez P (2004) Molecular quantification of lactic acid bacteria in fermented milk products using real-time quantitative PCR. *Int J Food Microbiol* 97(2):197–207.
8. Lance GN, Williams WT (1967) Mixed-data classificatory programs, I.) Agglomerative systems. *Aust Comput J* 1(1):15–20.
9. Hamady M, Lozupone C, Knight R (2010) Fast UniFrac: Facilitating high-throughput phylogenetic analyses of microbial communities including analysis of pyrosequencing and PhyloChip data. *ISME J* 4(1):17–27.
10. Dray S, Dufour AB (2007) The ade4 package: Implementing the duality diagram for ecologists. *J Stat Softw* 22(4):1–20.
11. Hazen TC, et al. (2010) Deep-sea oil plume enriches indigenous oil-degrading bacteria. *Science* 330(6001):204–208.
12. Storey JD, Tibshirani R (2003) Statistical significance for genomewide studies. *Proc Natl Acad Sci USA* 100(16):9440–9445.
13. Letunic I, Bork P (2007) Interactive Tree Of Life (iTOL): An online tool for phylogenetic tree display and annotation. *Bioinformatics* 23(1):127–128.
14. Letunic I, Bork P (2011) Interactive Tree Of Life v2: Online annotation and display of phylogenetic trees made easy. *Nucleic Acids Res* 39(Web Server issue):W475–W478.

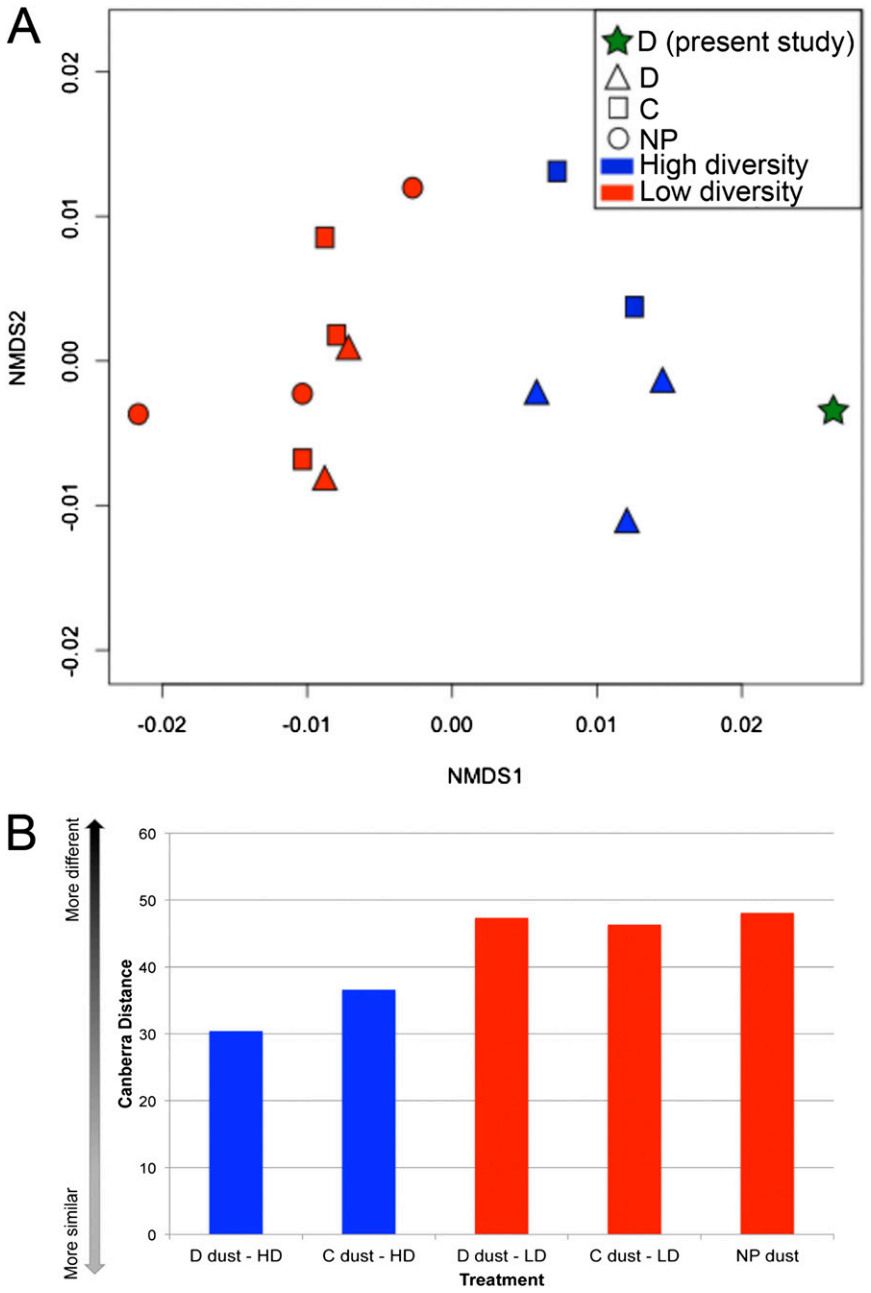

Fig. S1. (*A*) Dog (D)-associated house dust used for this study is compositionally more similar to other D-associated house dust samples. NMDS ordination reveals that the D-associated house dust used in this study exhibits greatest compositional similarity to other high diversity pet-associated house dust samples profiled in a previous study using the same platform. C, cat; D, dog; NP, no pet. (*B*) Calculated Canberra distances between the D dust sample used in this study and other samples previously profiled under identical conditions confirm that it is most similar to other high-diversity D dust samples (C, cat; D, dog; HD, high diversity; LD, low diversity; NP, no pet).

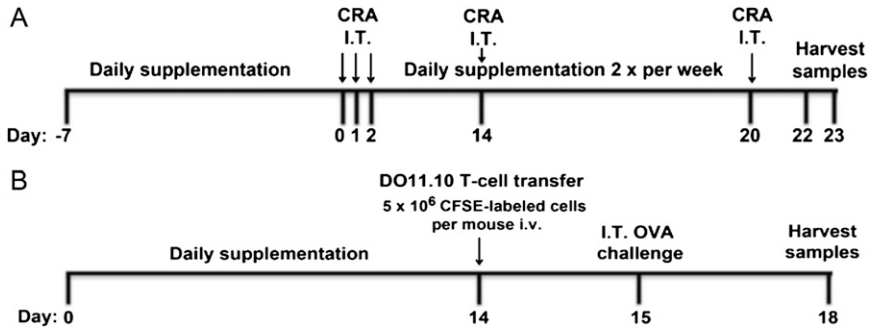

Fig. S2. Experimental design of murine models used in this study. (*A*) Cockroach allergen (CRA) airway challenge model involved daily oral gavage of mice (n = 5 per group) with D, NP dust suspension or saline before CRA sensitization via intratracheal administration. Animals in the control treatment group received no interventions. Following the initial CRA sensitization on day 7, animals continued to receive the relevant supplementation by oral gavage twice per week. During this period, mice were challenged on days 14, 20, and 22 with CRA, before the end of the protocol (EP) on day 23. (*B*) DO11.10 T-cell transfer OVA model was performed in a similar manner in that animals (n = 5 per group) received daily supplementation with D, NP dust suspension or saline for 14 d before transfer of naïve T cells and subsequent intratracheal OVA challenge on day 15. Animals were taken at the end of the protocol (EP) on day 18. Control animals received no treatment.

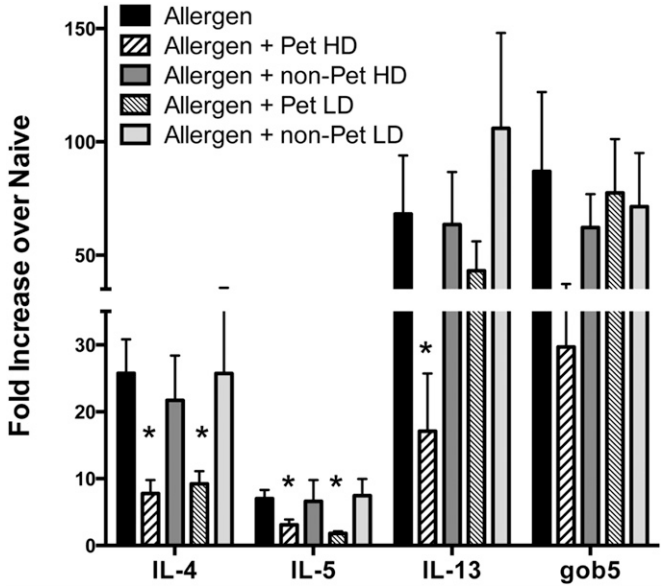

Fig. S3. Allergen-responsive phenotype is sustained despite normalization of house dust exposures. Animals were exposed to either equivalent high dose (HD) (25 mg) or low dose (LD) (6.25 mg) of dog- (D) or no-pet (NP)–associated house dust as described in *SI Materials and Methods*. Airway Th2 cytokine and *gob5* gene expression was quantified for each group. Reduced exposure to D-associated house dust still resulted in significant reductions in Th2 cytokine expression in the airways, although the reduction in *gob5* gene expression observed upon high level exposure to D dust, was lost upon reduced exposure. Increased exposure to NP-associated house dust did not result in reduced Th2 cytokine or *gob5* responses in murine airways.

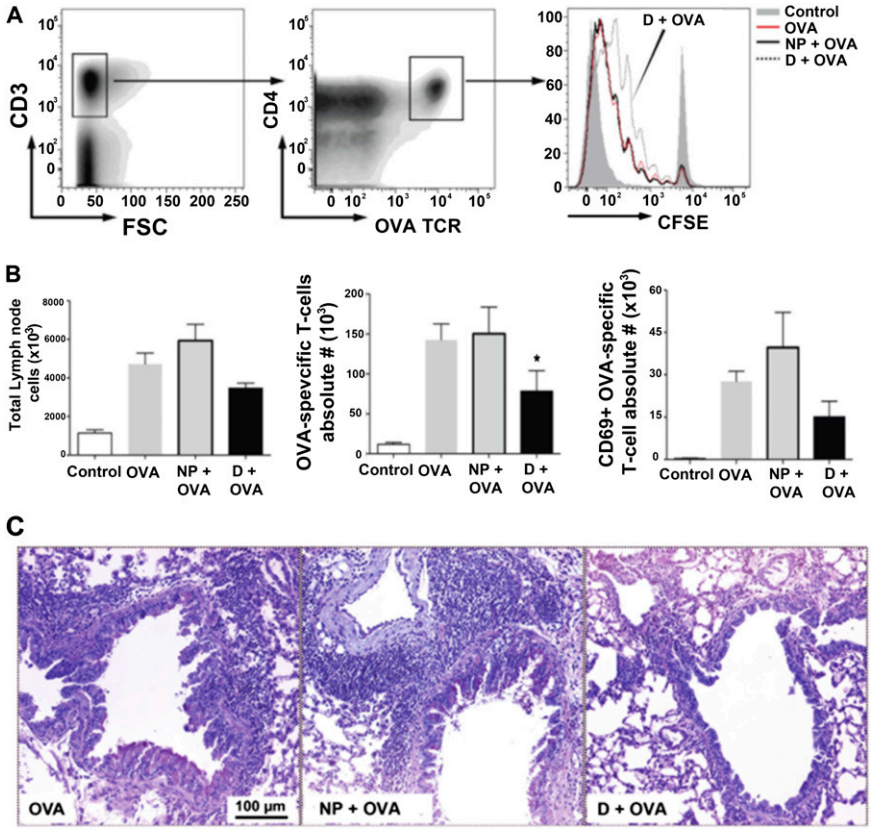

Fig. S4. Supplementation of dust from homes with dogs reduces antigen-specific T-cell expansion and pulmonary inflammation in a primary immune response. Using naïve DO.11 ovalbumin-specific transgenic TCR T-cell transfer into dust-supplemented and ovalbumin airway-challenged mice, studies examined the role of the effects of dust on initiation of the immune response. (*A*) CFSE-labeled T cells from DO.11 mice were tracked for their expansion using classic dilution of CFSE as a measure of proliferation and demonstrated a reduction in CFSE dilution in the D dust-supplemented mice. (*B*) Enumeration of total lymph nodes cells (*Left*), ovalbumin TCR-specific T cells (*Center*), and $CD69^{+}$ activated ovalbumin-specific TCR-specific T cells (*Right*) were all reduced in only the D dust-supplemented animals; * indicates $P < 0.05$. (*C*) The histologic examination of the peribronchial inflammation confirmed that D dust-supplemented animals displayed a significant reduction in the primary ovalbumin specific responses. Data represent the mean ± SE from five mice per group.

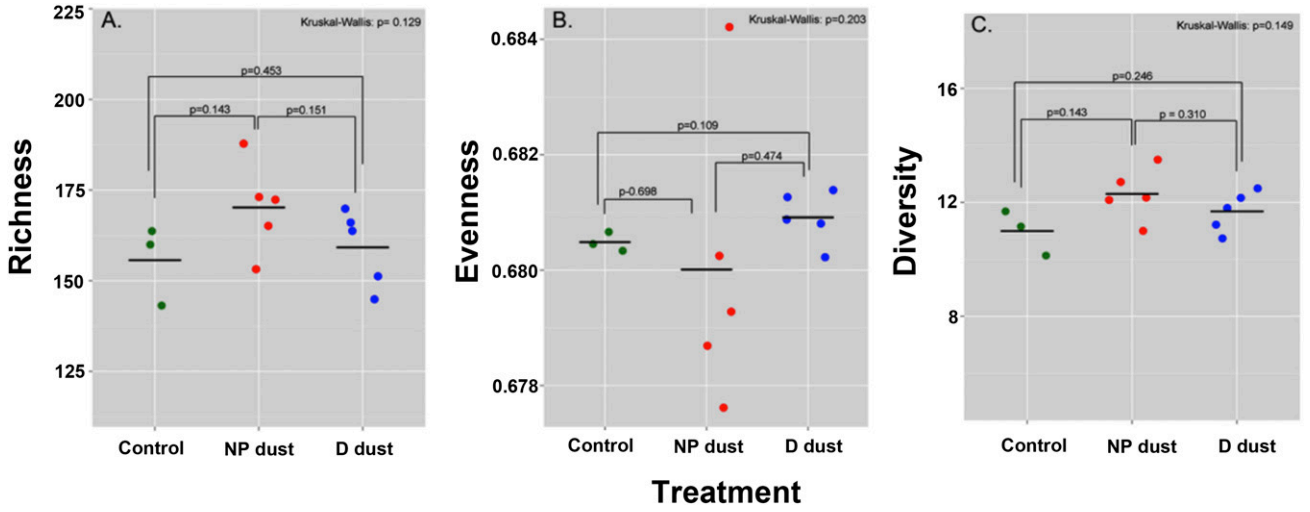

Fig. S5. Gross community metrics are not significantly altered across treatment groups used in this study. Microbial community richness (*A*), Pielou's evenness (*B*), and Faith's phylogenetic diversity (*C*), of cecal communities were not significantly different between control mice and those gavaged with NP dust or D dust.

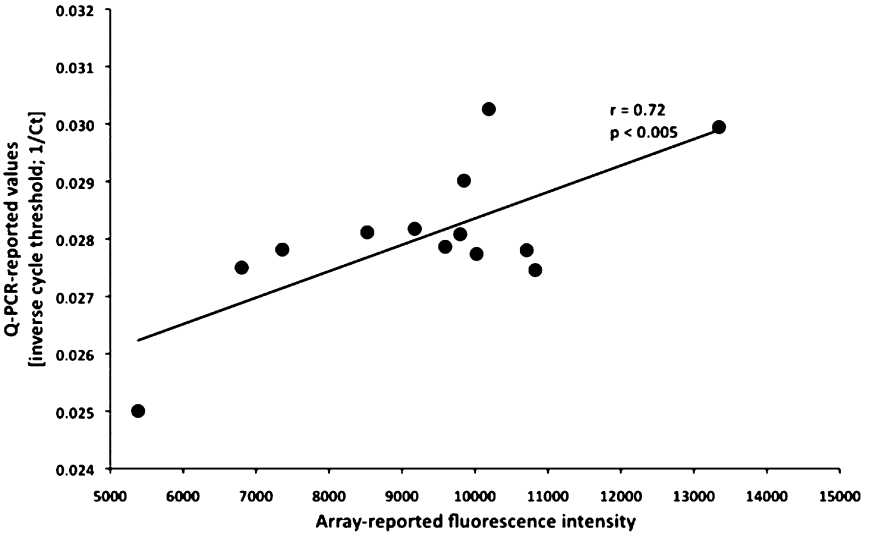

Fig. S6. Validation of array-based *L. johnsonii* relative abundance by independent Q-PCR. Regression analysis of inverse cycle threshold values plotted against array-reported fluorescence intensity for taxon 7028 was used to confirm the relative abundance of *L. johnsonii* in these samples.

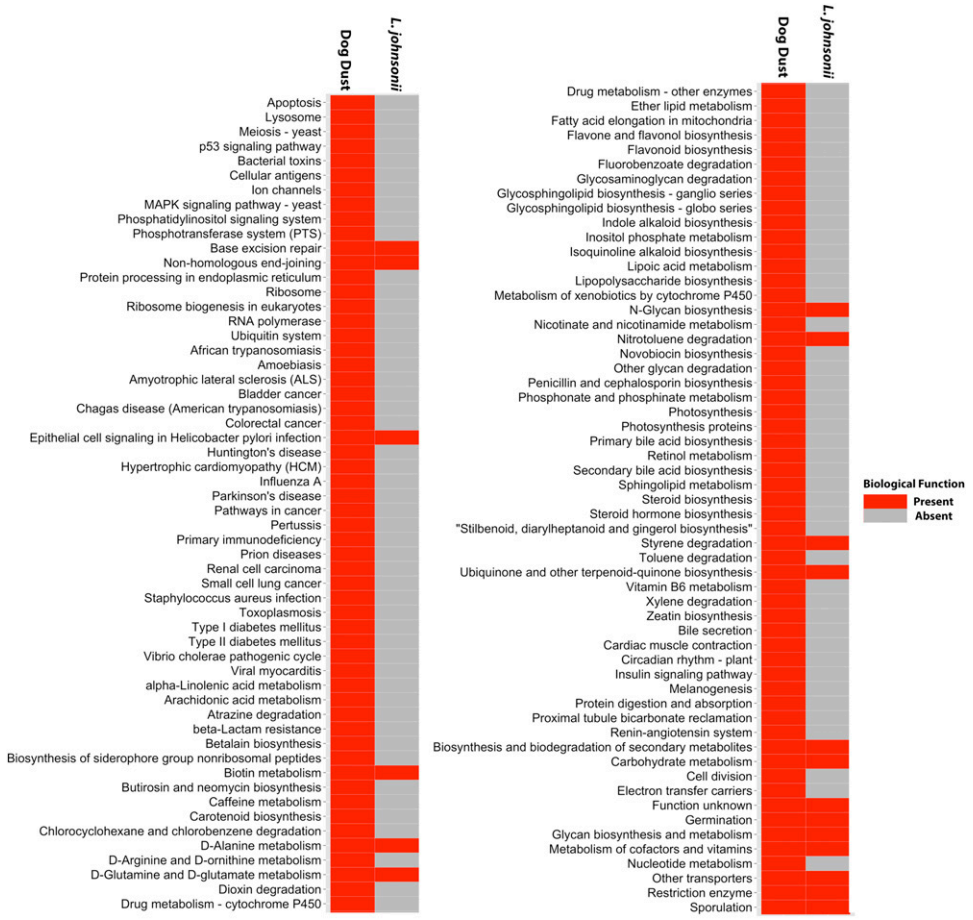

Fig. S7. D dust-exposed animals exhibit a broader range of predicted community function compared with *L. johnsonii*-supplemented animals. Heat map visualization of PICRUSt-predicted community metagenomes of D dust- and *L. johnsonii*-supplemented animals compared with respective controls. D dust-supplemented animals exhibit enrichment of an increased number of KEGG pathways compared with animals who received *L. johnsonii*. Common pathways enriched in both treatment groups include N-glycan biosynthesis and secondary metabolism pathways, implicating these and other shared KEGG pathways in the airway protective phenomenon observed across both treatment groups.

Table S1. Taxa significantly enriched in D-associated house dust-supplemented animals compared with control mice

Phylum	Family	Taxon ID	Representative species	Relative enrichment (FI)	*P* value	*q* value
Taxa enriched in D dust-supplemented animals						
Firmicutes	Lachnospiraceae	11084	Equine manure clone	5,165.57	3.40E-04	3.07E-02
Firmicutes	Peptococcaceae	4663	*Desulfosporosinus meridiei*	4,049.61	3.85E-02	1.38E-01
Firmicutes	Bacillaceae	5973	*Bacillus circulans*	3,141.76	1.82E-03	5.94E-02
Firmicutes	Lactobacillaceae	7028	*Lactobacillus gasseri (L. johnsonii)*	2,734.05	4.54E-02	1.44E-01
Proteobacteria	Pasteurellaceae	3343	*Actinobacillus rossii*	2,605.00	3.93E-02	1.39E-01
Firmicutes	Lachnospiraceae	11092	mpn-isolate group	2,378.85	4.23E-02	1.40E-01
Firmicutes	Lachnospiraceae	10380	*Dorea longicatena*	2,252.60	1.52E-02	9.81E-02
Firmicutes	Ruminococcaceae	10132	Rumen clone	2,217.02	2.42E-03	5.94E-02
Firmicutes	Clostridiaceae	9826	*Clostridium uliginosum*	2,159.64	9.51E-03	7.75E-02
Firmicutes	Paenibacillaceae	7001	*Paenibacillus* sp.	2,139.13	2.45E-03	5.94E-02
BRC1	Unclassified	1366	Penguin droppings clone	2,027.62	1.24E-02	8.62E-02
Firmicutes	Lactobacillaceae	5507	*Lactobacillus gallinarum*	1,920.70	1.75E-02	1.01E-01
Cyanobacteria	Unclassified	8314	Microbial mat	1,818.16	6.04E-03	7.10E-02
Firmicutes	Lachnospiraceae	10118	Rumen clone	1,784.85	4.38E-02	1.43E-01
Unclassified	Unclassified	1954	*Thermodesulfobium narugense*	1,737.58	2.16E-03	5.94E-02
Firmicutes	Lactobacillaceae	6107	*Lactobacillus ferintoshensis*	1,652.91	4.42E-02	1.43E-01
Acidobacteria	Acidobacteriaceae	8372	PCB-polluted soil clone	1,588.71	4.34E-03	6.63E-02
Firmicutes	Lachnospiraceae	10371	Vaginal lavage	1,584.88	1.87E-02	1.01E-01
Firmicutes	Lachnospiraceae	9918	Gulf Mexico clone	1,576.20	8.35E-03	7.43E-02
Firmicutes	Leuconostocaceae	5813	*Weissella cibaria*	1,573.64	2.80E-03	6.12E-02
Firmicutes	Bacillaceae	5842	*Streptococcus pyogenes*	1,563.35	1.14E-02	8.19E-02
WPS-2	Unclassified	2625	Volcanic deposit clone	1,559.73	2.95E-03	6.12E-02
Firmicutes	Lactobacillaceae	6524	*Lactobacillus kitasatonis*	1,558.53	4.13E-02	1.39E-01
Bacteroidetes	RikenellaceaeII	7504	Cow rumen clone	1,539.98	2.01E-02	1.01E-01
Proteobacteria	Desulfobacteraceae	8147	Hypersaline lake clone	1,519.96	6.15E-03	7.10E-02
Firmicutes	Lactobacillaceae	5839	*Lactobacillus antri*	1,495.99	2.46E-02	1.07E-01
Proteobacteria	Vibrionaceae	2494	*Vibrio logei*	1,488.82	4.49E-02	1.44E-01
Firmicutes	Bacillaceae	6379	*Bacillus cereus*	1,487.01	4.50E-02	1.44E-01
Firmicutes	Clostridiaceae	10661	*Clostridium josui*	1,482.40	2.09E-02	1.01E-01
Firmicutes	Lachnospiraceae	11041	Biodegraded Canadian oil reservoir clone	1,456.64	1.96E-02	1.01E-01
Proteobacteria	Rhodospirillaceae	7752	Deep sea sediment clone	1,369.28	5.07E-03	7.10E-02
Spirochaetes	Spirochaetaceae	6229	*Spirochaeta taiwanensis*	1,349.26	3.21E-02	1.24E-01
Proteobacteria	Caulobacteraceae	8887	*Brevundimonas diminuta*	1,316.16	1.70E-02	1.01E-01
Actinobacteria	Micromonosporaceae	1539	*Micromonospora eburnea*	1,295.54	7.90E-03	7.43E-02
Firmicutes	Paenibacillaceae	5820	*Bacillus* sp.	1,272.28	3.00E-03	6.12E-02
Actinobacteria	Microbacteriaceae	1458	Freshwater clone	1,264.87	2.30E-02	1.04E-01
Firmicutes	Ruminococcaceae	9896	Herbivore gastrointestinal tract clone	1,235.24	1.62E-02	9.92E-02
Firmicutes	Lachnospiraceae	9691	*Ruminococcus* sp.	1,140.28	1.76E-02	1.01E-01
Cyanobacteria	Pseudanabaenaceae	8597	*Synechococcus* sp.	1,055.75	3.05E-02	1.22E-01
Proteobacteria	Thiotrichaceae	4886	Marine sediment clone	1,052.44	2.35E-02	1.04E-01
Acidobacteria	Acidobacteriaceae	5485	Uranium mining tailing clone	1,050.05	8.89E-03	7.58E-02
Proteobacteria	Phyllobacteriaceae	7632	Cultivating Sargasso clone	1,017.70	2.18E-02	1.03E-01
Acidobacteria	Solibacteraceae	5527	Water 10 m downstream clone	994.26	7.27E-03	7.26E-02
Proteobacteria	Chromatiaceae	3880	Mid-Atlantic Ridge clone	991.00	3.60E-02	1.36E-01
Firmicutes	Lactobacillaceae	6923	*Lactobacillus vaginalis*	967.24	6.66E-04	3.07E-02
Firmicutes	Bacillaceae	5594	*Bacillus megaterium*	963.27	6.46E-03	7.10E-02
Proteobacteria	Rhodospirillaceae	8788	*Tistrella mobilis*	928.57	6.49E-03	7.10E-02
Actinobacteria	Micromonosporaceae	1337	*Micromonospora fulviviridis*	911.10	4.07E-02	1.39E-01
Actinobacteria	Micromonosporaceae	1030	*Micromonospora chaiyaphumensis*	905.11	1.90E-02	1.01E-01
Proteobacteria	Piscirickettsiaceae	2759	*Piscirickettsia salmonis*	904.38	2.13E-02	1.02E-01
Firmicutes	Bacillaceae	6292	*Bacillus pallidus*	871.75	8.39E-03	7.43E-02
Deferribacteres	Calithrixaceae	4360	*Caldithrix abyssi*	781.45	4.24E-03	6.63E-02
Firmicutes	Ruminococcaceae	10838	*Acetanaerobacterium elongatum*	736.62	5.58E-03	7.10E-02
Proteobacteria	Xanthomonadaceae	4650	*Xylella fastidiosa*	734.34	2.98E-02	1.20E-01
Acidobacteria	Acidobacteriaceae	6679	Uranium mining trailing clone	686.77	3.73E-02	1.38E-01
Proteobacteria	Pseudomonadaceae	2887	*Pseudomonas fluorescens*	682.23	3.83E-02	1.38E-01
Firmicutes	Paenibacillaceae	7035	Hot Springs clone	677.25	1.30E-02	8.95E-02
Actinobacteria	Micromonosporaceae	399	*Micromonospora chersinia*	670.20	2.41E-02	1.06E-01
Firmicutes	Paenibacillaceae	5566	*Paenibacillus* sp.	639.02	4.44E-04	3.07E-02
Actinobacteria	Micromonosporaceae	1285	*Micromonospora* sp.	605.18	1.13E-02	8.19E-02
Chloroflexi	Chloroflexaceae	9502	Forest soil clone	599.26	3.08E-02	1.22E-01

Table S1. Cont.

Phylum	Family	Taxon ID	Representative species	Relative enrichment (FI)	*P* value	*q* value
Bacteroidetes	Flexibacteraceae	2854	*Flexibacter flexilis*	589.79	1.53E-02	9.81E-02
Actinobacteria	Cellulomonadaceae	1309	Lichen-dominated Antarctic	562.47	1.06E-02	7.96E-02
Firmicutes	Bacillaceae	6870	*Bacillus megaterium*	525.29	2.83E-02	1.16E-01
Proteobacteria	Thiotrichaceae	3753	Indian Ocean clone	516.71	9.92E-03	7.75E-02
Firmicutes	Bacillaceae	5400	*Bacillus niacini*	504.09	1.87E-02	1.01E-01
Firmicutes	Bacillaceae	7076	*Bacillus smithii*	496.67	2.95E-05	1.36E-02
Actinobacteria	Micromonosporaceae	806	*Micromonospora inositola*	482.10	1.62E-03	5.94E-02
Proteobacteria	Bradyrhizobiaceae	9747	*Oligotropha carboxidovorans*	439.67	3.15E-02	1.24E-01
Proteobacteria	Sinobacteraceae	3726	Soil near uranium tailings clone	331.33	2.35E-02	1.04E-01
Actinobacteria	Microbacteriaceae	802	*Microbacterium phyllosphaerae*	316.66	2.52E-02	1.07E-01
Actinobacteria	Microbacteriaceae	214	*Microbacterium liquefaciens*	315.32	3.49E-02	1.33E-01
Actinobacteria	Micromonosporaceae	1543	*Micromonospora purpurea*	313.28	1.04E-02	7.96E-02
Firmicutes	Bacillaceae	6208	*Geobacillus stearothermophilus*	311.48	6.47E-04	3.07E-02
Actinobacteria	Micromonosporaceae	1260	*Micromonospora echinospora*	308.37	4.09E-02	1.39E-01
Actinobacteria	Micromonosporaceae	748	*Micromonospora* sp.	283.75	4.25E-02	1.40E-01
Firmicutes	Bacillaceae	5512	*Bacillus aquimaris*	250.50	9.77E-03	7.75E-02
Firmicutes	Unclassified	4632	Thermophilic anaerobic clone	235.27	4.46E-03	6.63E-02
Proteobacteria	Burkholderiaceae	5314	*Burkholderia glathei*	208.57	2.00E-02	1.01E-01
Actinobacteria	Microbacteriaceae	269	*Agromyces neoliticus*	180.09	2.20E-02	1.03E-01
Actinobacteria	Nocardiaceae	1751	*Skermania piniformis*	130.48	1.47E-02	9.81E-02
Proteobacteria	Pseudomonadaceae	1984	*Pseudomonas alcaligenes*	125.54	3.73E-03	6.14E-02
Firmicutes	Enterococcaceae	6242	*Enterococcus faecium*	116.93	2.21E-03	5.94E-02
Proteobacteria	Halomonadaceae	2997	*Halomonas alimentaria*	111.57	5.88E-03	7.10E-02
Proteobacteria	Bradyrhizobiaceae	9305	*Afipia massiliensis*	105.59	2.07E-03	5.94E-02
Proteobacteria	Pseudomonadaceae	2786	*Pseudomonas alcaligenes*	97.97	1.77E-02	1.01E-01
Actinobacteria	Frankiaceae	186	*Frankia* sp	91.19	2.08E-02	1.01E-01
Proteobacteria	Halomonadaceae	2007	*Halomonas salina*	82.71	8.32E-03	7.43E-02
Proteobacteria	Pseudomonadaceae	2779	*Pseudomonas japonica*	77.36	3.22E-02	1.24E-01
Proteobacteria	Comamonadaceae	5250	Hindgut homogenate larva clone	73.52	1.65E-02	1.00E-01
Proteobacteria	Xanthomonadaceae	4257	*Stenotrophomonas maltophilia*	71.05	9.93E-03	7.75E-02
Firmicutes	Bacillaceae	5425	*Geobacillus stearothermophilus*	68.79	2.53E-02	1.07E-01
Actinobacteria	Streptomycetaceae	476	*Streptomyces griseoruber*	63.97	5.81E-03	7.10E-02
Actinobacteria	Micromonosporaceae	216	*Micromonospora echinospora*	61.97	7.41E-03	7.26E-02
Actinobacteria	Micromonosporaceae	1797	*Micromonospora* sp.	56.34	8.87E-03	7.58E-02
Actinobacteria	Cellulomonadaceae	1559	Lichen-dominated Antarctic clone	56.20	2.03E-02	1.01E-01
Proteobacteria	Burkholderiaceae	4718	*Burkholderia pseudomallei*	43.41	5.99E-03	7.10E-02
Actinobacteria	Nocardioidaceae	1515	*Nocardioides oleovorans*	40.81	3.59E-03	6.12E-02
Firmicutes	Bacillaceae	6139	*Bacillus amyloliquefaciens*	38.91	1.23E-02	8.62E-02
Proteobacteria	Methylobacteriaceae	10767	*Methylobacterium organophilum*	31.03	3.35E-03	6.12E-02
Proteobacteria	Rhodobacteraceae	3358	*Rhodovulum* sp.	23.75	3.25E-02	1.25E-01
Actinobacteria	Microbacteriaceae	861	*Agromyces ramosus*	17.39	1.54E-02	9.81E-02
Actinobacteria	Nocardiaceae	1166	*Rhodococcus equi*	12.70	3.73E-02	1.38E-01
Proteobacteria	Sphingomonadaceae	8332	Drinking water simulator clone	11.70	2.21E-03	5.94E-02

Table S2. Taxa significantly enriched in *L. johnsonii*-supplemented or control animals

Phylum	Family	Taxon ID	Representative species	*ΔFI	*P* value	*q* value
Taxa enriched in *L. johnsonii*-supplemented animals						
Bacteroidetes	RikenellaceaeII	8246	Rumen clone F23-G06	3,708.6	0.018	0.118
Bacteroidetes	RikenellaceaeII	8028	Cow rumen clone	2,369.6	0.031	0.151
Proteobacteria	Hyphomicrobiaceae	7336	Candidatus *Devosia euplotis*	2,273.7	0.001	0.034
Caldiserica	062DZ04	9683	Temporal variation Spirochetal	2,213.7	0.01	0.095
Firmicutes	Ruminococcaceae	9995	*Ruminococcus* sp. str.	1,504.5	0.001	0.034
Bacteroidetes	RikenellaceaeII	8923	Temperate estuarine mud	1,470.8	0.005	0.067
Bacteroidetes	Flammeovirgaceae	1914	Marine isolate str.	1,415.4	0.001	0.034
Bacteroidetes	Flammeovirgaceae	2574	Marine sediment clone	1,398	0.005	0.067
Firmicutes	Desulfitobacteraceae	4420	Endosymbiont *Trimyema*	1,092	0.021	0.123
Spirochaetes	Spirochaetaceae	6229	*Spirochaeta taiwanensis*	958.5	0.012	0.097
Cyanobacteria	Nostocaceae	7732	*Anabaena spiroides*	837.1	0.008	0.083
Taxa enriched in control animals						
Firmicutes	Lachnospiraceae	9843	Rumen clone F24-A02	−2,122.5	0.018	0.118
Firmicutes	Lachnospiraceae	10861	Rumen clone F23-B10	−1,830.8	0.001	0.034
Firmicutes	Ruminococcaceae	11017	*Bacteroides capillosus* str.	−1,402.5	0.013	0.102
Chloroflexi	Unclassified	1660	Uranium mining waste	−1,392.0	0.004	0.064
Cyanobacteria	Nostocaceae	8002	*Anabaena* flos-aquae	−1,242.5	0.021	0.123
Planctomycetes	Unclassified	431	Cultivating Sargasso Sea	−1,017.2	0.046	0.201
Firmicutes	Lachnospiraceae	10892	*Clostridium* sp. str.	−1,000.6	0.040	0.181
LCP-89	Unclassified	3812	Saltmarsh clone LCP-89	−920.8	0.007	0.083
Proteobacteria	Hyphomicrobiaceae	9768	*Hyphomicrobium aestuarii*	−741.5	0.026	0.134
Proteobacteria	Rhodocyclaceae	5223	*Thauera chlorobenzoica*	−557.8	0.024	0.127

*Taxon mean fluorescent intensity differential between treatment groups (*L. johnsonii*-supplemented animals minus unsupplemented control mice).